JOURNAL OF MATERIALS SCIENCE 22 (1987) 581–586

Shock compaction of NiTi alloy powder

HITOSHI MATSUMOTO*‡, KEN-ICHI KONDO*, SHOSO DOHI§, AKIRA SAWAOKA*
*Research Laboratory of Engineering Materials, Tokyo Institute of Technology, 4259 Nagatsuta, Midori, Yokohama 227, Japan
§Department of Applied Physics, The National Defense Academy, 10-20, Hashirimizu 1 chome, Yokosuka 239, Japan

The shock recovery experiment for the equiatomic NiTi alloy powder was performed by the flyer impact technique. The powder samples with the initial density of 70% of full density were shock-treated in the flyer velocity range 0.65 to 1.7 km sec^{-1}. At the optimum flyer velocity of 1.3 km sec^{-1}, the powder sample is compacted up to 99.5% of the full density. With increasing flyer velocity, new pores are formed in the melted layer instead of the disappearance of initial interstices. Effects of the mechanical deformation and the annealing brought by the shock treatment evidently appear in the temperature dependence of electrical resistivity accompanied with the martensitic transformation. The shock state and the relaxation of the heterogeneous temperature by the shock treatment are estimated, which indicate the annealing condition caused by shock-loading and the formation of new pores.

1. Introduction

Although hot forming techniques such as hot-pressing and hot extrusion are usually employed for powder compaction, a shock compaction technique utilizing shock waves has recently been developed. In particular, the application of a shock compaction technique is useful for materials which are difficult to compact, amorphous materials and so on, because the shock wave propagation in powder brings out high pressure during a period of microseconds, and high temperatures near the interface of powder which cause intergranular binding. Investigations of the basic effect of shock waves on porous materials have been carried out on standard powders such as copper, iron and stainless steel powder in order to clear the state during shock compression and the residual effects after the passage [1–7]. However, the mechanism of powder consolidation has not yet been satisfactorily elucidated, because the interaction between powder and shock wave is complicated, depending on mechanical and physical properties of material such as strength, ductility, specific heat, melting temperature, thermal conductivity, etc.

For a better understanding of the shock compaction phenomena, it is helpful to utilize a unique property of a material which makes it possible to characterize the shock effect. In this paper, the equiatomic nickel–titanium alloy is employed, which has the specific feature of a shape memory attributed to the thermoelastic martensitic transformation around room temperature. The shock recovery experiment on the powder of NiTi alloy was carried out by using a powder gun, in order to observe the microstructure and to measure the electrical resistivity near the transition temperature after shock loading.

2. Experimental details

The NiTi alloy powder used as a starting material was supplied by Daido Special Steel Co. Ltd (Minami, Nagoya, Japan). The powder was prepared by a centrifugal atomizing method. The powder particles were generally spherical in the range of about 50 to 200 μm in diameter. The X-ray diffraction results at room temperature indicated the low temperature phase which was considered as a monoclinic system [8, 9]. The shock recovery experiment was performed by a flyer plate impact technique, using the powder gun (HS-3C, Tokyo Institute of Technology) which was a modified apparatus of the two-stage light-gas gun (HS-3B) [10]. The alloy powder was pressed into a copper capsule, as shown in Fig. 1. The capsule was sealed by a copper plug and solder in a vacuum and was held in a mild-steel holder bonded with the momentum-trap of a metal block. The sample space in the capsule was 10 mm in diameter and 4 mm thick, and the relative density of the charged sample was 70 $\pm$ 5%. The copper capsule was 20 mm in outside diameter and 10 mm in height. Two types of mild-steel holder were used, corresponding to the flyer velocity. For the flyer velocities under 1 km sec^{-1}, one was 70 mm in diameter and 30 mm in height with a hole into which the capsule is just put, as shown in Fig. 1a. For the higher velocities, the other was 40 mm in height with a deeper hole of 10 mm and the capsule was set up at the hole bottom in order to reduce the deformation of the sample, as shown in Fig. 1b. The flyer consisted of an impactor of a copper disc with dimensions of 20 mm in diameter and 1.5 mm in thickness and a sabot formed by a cylinder of resin and a lead foil, as shown in Fig. 1. This lead foil was inserted in the sabot for the definite measurement of the flyer

‡*Present address*: Department of Applied Physics, The National Defense Academy, 10–20 Hashirimizu 1 chome, Yokosuka 239, Japan.

0022–2461/87 $03.00 + .12

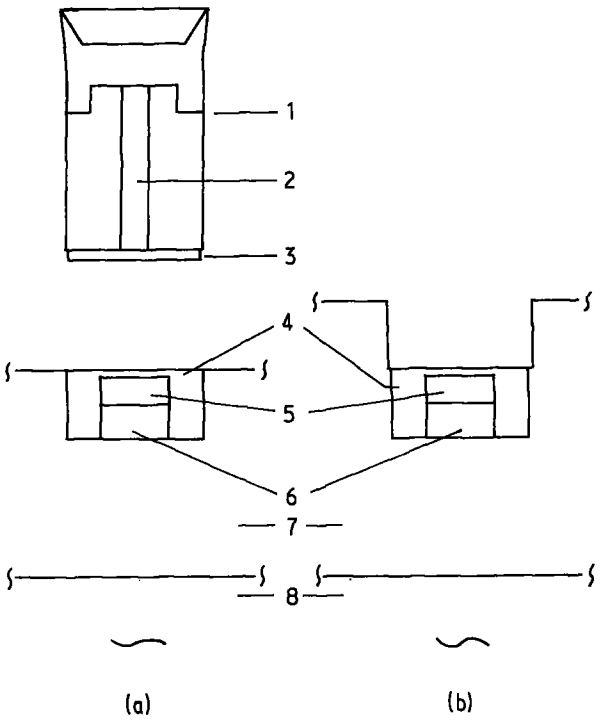

Figure 1 Cross-section of flyer and shock recovery assemblies. (a) flyer velocities under 1 km sec^{-1}, (b) higher velocities. 1, flyer sabot; 2, lead foil; 3, impactor; 4, copper capsule; 5, sample; 6, copper plug; 7, mild-steel holder; 8, momentum trap.

velocity using X-rays. Details for the velocity measurement apparatus and the gun used are presented elsewhere [10]. In the present experiment, the flyer velocity was in the range of 0.65 to 1.7 km sec^{-1}, for which the generated shock pressure in the sample was in the range of 4.2 to 20 GPa, as described below.

The apparatus density of the recovered sample was measured by an Archimedean method. The shock-treated sample was halved by using a crystal-cutter equipped with a SiC blade, and the cross-section of the bisectional sample was polished with polishing papers of SiC and with diamond paste on a cloth. The polished surface was etched in a solution of H_2O : HNO_3 : HF = 40 : 1 : 3 and then the microstructure was observed under a metallurgical microscope. The specimen for the electrical resistivity measurement was cut off from the central portion of the shock-treated sample. The electrical resistivity was measured by a standard four-probe potentiometric method in the temperature range of about 150 to 420 K at a thermal cycle rate of 0.5 K min^{-1}. The temperature was measured within the relative accuracy of 0.1 K by using the Copper–Constantan thermocouple spot-welded to the specimen. The relative accuracy in the electrical resistivity measurement caused by the temperature measurement was estimated to be within $\pm 0.05\%$. The error, occurring principally from the specimen dimensions, was of the order of $\pm 5\%$. Corrections for the temperature difference between both ends of the specimen were considered, whereas the thermal expansion was neglected.

3. Estimation of shock state

It has been found that the Hugoniot relations of many materials can be adequately represented by a linear relationship between the shock velocity (U_s) and the particle velocity (U_p) [11]. It is assumed in the present calculation that the U_s–U_p relationship for the solid NiTi alloy can be expressed by averaging the measured values for pure Ti and pure Ni as follows

$$U_s = 4.901 + 1.115\,U_p \ (\mathrm{km\,sec^{-1}}) \qquad (1)$$

as no measurement is made on the NiTi alloy. Using this equation, the Rankine–Hugoniot equations and the Mie–Grüneisen equation of state, the Hugoniot relation for the porous material can be calculated when coupled with the known initial conditions and the Grüneisen parameter (γ) [12]. In the present study, the relative packing density is 70% and the density of the solid NiTi alloy is $6.45 \times 10^3\,\mathrm{kg\,m^{-3}}$. The initial pressure is negligible. The volume-dependence of the γ was evaluated as follows

$$\frac{\gamma}{V} = \frac{\gamma_0}{V_0} \qquad (2)$$

where V is the volume and the zero subscript refers to the initial state. This approximation is usually reasonable in shock data analysis. The γ_0 was calculated at 1.30 by using the thermodynamic relationship,

$$\gamma = \frac{VK_T\alpha}{C_v} \qquad (3)$$

where K_T is the isothermal bulk modulus, α is the coefficient of volume expansion and C_v is the specific heat at constant volume [13–15]. The values of parameters such as the shock pressure, P, the volume, V and the internal energy, E for the Hugoniot relation under the present shock conditions were determined by the impedance match method using the calculated Hugoniot relation of porous NiTi alloy and the published Hugoniot relation of copper [11].

Total energy (E_T) deposited during shock loading was actually estimated by the following equations which referred to the isotherm at the initial temperature and the Mie–Grüneisen equation of state

$$E_T = E + \int_{V_0}^{V} P_K\,\mathrm{d}V \qquad (4)$$

$$P - P_K = \frac{E_T\gamma}{V} \qquad (5)$$

where subscript K presents the isentropic compression state at volume V. The variable P_K was eliminated from these equations, and the value of E_T was calculated numerically from the resulting integral equation. The shock temperature (T_s) was obtained by converting the deposited energy E_T into the temperature on the basis of the Debye model for the thermal energy, where the initial Debye temperature $\theta_0 = 375$ K [13]. The volume-dependence of the Debye temperature, the latent heat from 0 K to the initial temperature and transformation heat to the high temperature phase [16] were considered in this calculation. The residual temperature (T_r) after the decay of shock pressure was estimated from the residual energy (E_r) as well as the shock temperature, where it was assumed that the shock state was relieved along the P–V Hugoniot of porous NiTi alloy. Fig. 2 shows the calculated results of the shock pressure P, the shock temperature

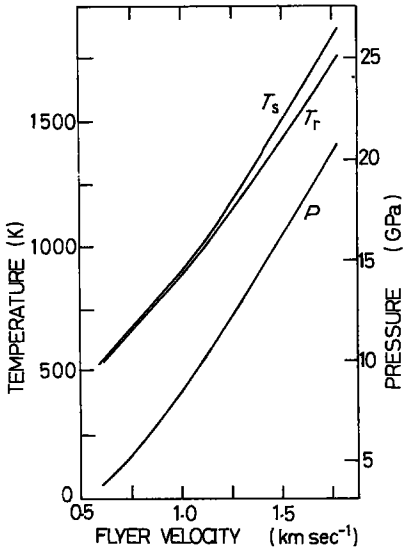

Figure 2 Shock pressure (P), shock temperature (T_s) and residual temperature (T_r) as a function of flyer velocity.

T_s and the residual temperature T_r as a function of flyer velocity. The difference between the T_s and T_r is negligible within 5% for the present powder sample.

4. Results and discussion

An appropriate flyer velocity is present for the compaction of the NiTi powder at a given apparent density. At the optimum flyer velocity of 1.3 km sec^{-1}, the powder sample is compacted up to 99.5% of the full density. The shock state is estimated to be at the shock pressure of 13 GPa and the shock temperature of 1240 K, as shown in Fig. 2.

Typical optical micrographs are seen in Fig. 3, showing features of voids and cracks in the shock-loaded samples at the flyer velocity of 0.65, 1.3 and 1.7 km sec^{-1}. In the series of photographs the residual pores seem to prevent the perfect aggregation of the NiTi powder sample. Although the density of the shock-recovered sample can be principally determined by the volume of pores, the pores exhibit different features, depending on the flyer velocity. Therefore, the shock condition for the compaction is divided into two regions by the features of the pores as follows: at the low flyer-velocity as shown in Fig. 3a, the porous sample does not achieve an intergranular bonding, and initial voids remain on the particle surface, whereas at the high flyer-velocity beyond the optimum velocity, new voids and cracks are formed in the melted zone instead of the disappearance of initial interstices, as shown in Fig. 3b.

The microstructures at the circumference of the recovered samples are directly influenced by the difference of the shock impedances between the powder sample and the copper capsule and by three-dimensional deformation during the shock loading as follows: an excessive shock wave reflects into the powder sample from the inner side of the copper capsule with a higher shock impedance and interacts with a direct plane shock wave so as to produce a long fissure with melted edges along the bottom of the recovered sample. The fissure for a flyer velocity of 1.3 km sec^{-1} is shown in Fig. 4. The three-dimensional deformation, in addition to the uniaxial deformation for the shock compaction, generates heat during the shock loading so as to bring about a melting. As shown in Fig. 5, such as melting can be obviously observed at the peripheral part in the remarkably deformed sample at the flyer velocity of 1.7 km sec^{-1}, but this effect is negligible for the melting structures at the flyer velocities of 0.65, 1.0 and 1.3 km sec^{-1}. Although these two effects are charcteristic of the sample assembly used here, the central area of the recovered samples except for the sample obtained at a flyer velocity of 1.7 km sec^{-1} is not strongly influenced and then compacted with a uniaxial deformation where the basic theory of shock wave can be applicable.

A relatively large amount of energy generated by the shock-loading is heterogeneously expanded at the surface regions of particles due to melting. The two temperatures calculated in Section 3 show the mean

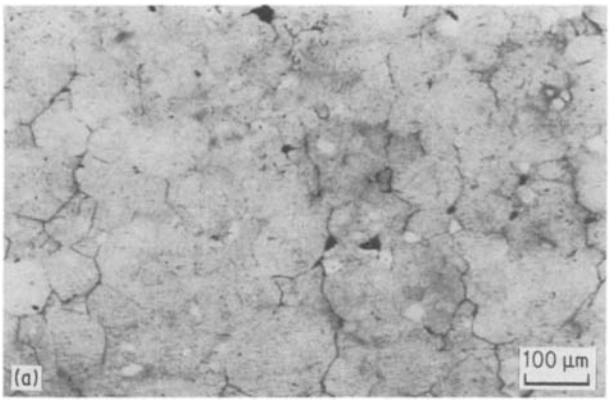

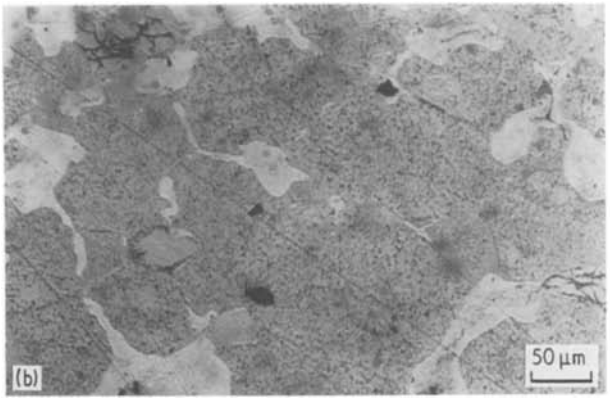

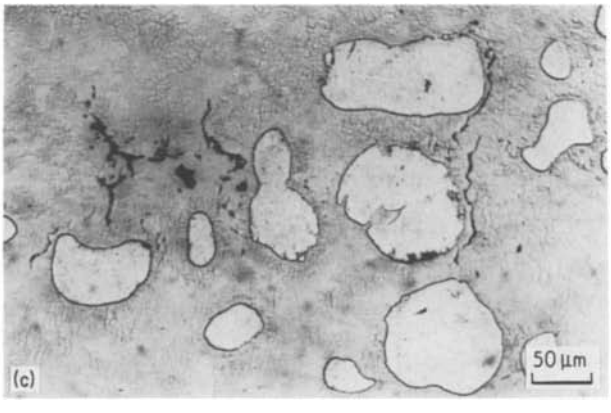

Figure 3 Microstructures of shock-loaded samples. Flyer velocities (a) 0.65, (b) 1.3 and (c) 1.7 km sec^{-1}.

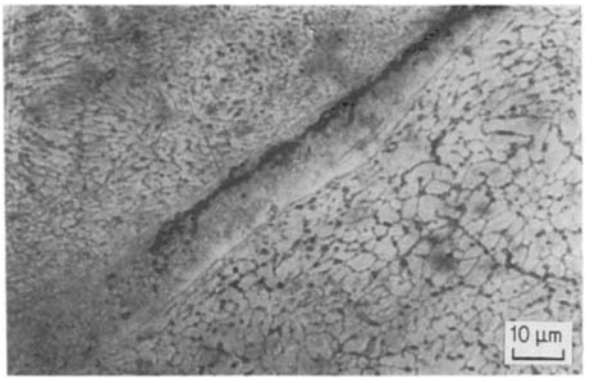

Figure 4 Optical micrograph of the fissure produced by the interaction between shock waves which is impacted at a flyer velocity of 1.3 km sec^{-1}.

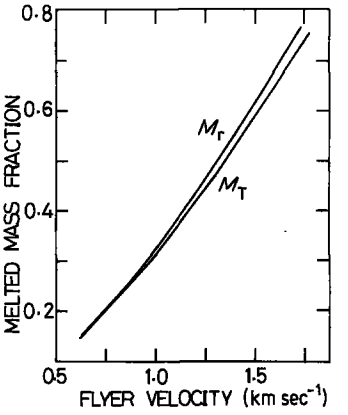

Figure 6 Calculated results of melted mass fractions M_T and M_r as a function of flyer velocity. The M_T and M_r are calculated on the basis of the total energy (E_T) deposited during shock loading and the residual energy (E_r) after the decay of shock pressure.

values on the whole of a sample. Therefore, the melted mass fraction can be approximated by regarding all of the deposited energy E_T or E_r as the thermal energy for melting. In this approximation, an upper bound to the melted mass fraction can be calculated, because the diffusion of the heat and the other energy transported directly into the interiors of powder particles are neglected in the shock process. Estimating the volume-dependence of the melting temperature by the Kennedy–Kraut equation [17, 18] and the thermal lattice energy up to the melting temperature by the Debye model, the maximum value of the melted mass fraction is calculated as a function of the flyer velocity, as shown in Fig. 6. Here the initial value of the melting temperature is 1550 K which is experimentally determined [19] and the latent heat of fusion is presumed to be 275 kJ kg^{-1} which is estimated from the relationship between the latent heat of fusion and the melting temperature for the metallic elements [20]. The difference between the melted mass fractions M_T and M_r based on the E_T and the E_r, respectively, is small. Even if the volume-dependences of the Debye temperature and the melting temperature are neglected, the calculated values fit each other within an error of 6%. The melted mass fractions for Figs 3a and b, which are determined by the area ratio of the melted region, are 0.07 and 0.23, respectively. The calculated values for the melted mass fraction are in qualitative agreement with the experimental results except for the sample shock-loaded at the highest velocity, but are roughly double the measured values. On the other hand, this calculation for the highest velocity is considered as a better approximation in quality, because the experimental value is asymptotic towards the calculated value or the upper limit with a decrease in the unmelted region which behaves as a heat sink and a reservoir of the other energy. The peripheral part in the sample shock-treated at the highest velocity, however, melts beyond the upper limit. This implies that the three-dimensional plastic deformation generates heat comparable to the uniaxial shock wave. Therefore, it is important to relate the melting structure with the marked plastic deformation.

The duration time (t_d) of shock state under the best compacting conditions is of the same order as the solidification time (t_s) of the melted layer because of the small thermal conductivity of NiTi alloy [13]. The t_d is estimated by adopting the shock velocity of solid as a velocity of rarefaction and the t_s is calculated from the equation

$$t_s = 0.013 \times h^2 \ (\mu\text{sec}) \qquad (6)$$

where h is the thickness of melted layer in unit of μm [21, 22]. Therefore, it is seen that the cracks and voids are critically produced in the melted region because of the high temperature of state during the solidification. For decreasing such cracks and voids, it is necessary to restrict the distribution of the thickness of the melted layer by using particles of the same size. Moreover, it will be effective to employ smaller particles since thickness of the melted region diminishes because of the increase of surface area, in comparison with increasing the shock duration time by using a thicker impactor.

Fig. 7 shows the temperature dependence of electrical resistivity for the shock-recovered samples at the flyer velocities of 0.65, 1.0 and 1.3 km sec^{-1}. The resistivity peak appears on cooling and also on heating except for the specimen shock-loaded at the flyer velocity of 1.3 km sec^{-1}. The temperature region for the transformation hysteresis increases as the flyer velocity decreases. The temperature width for the transformation spreads over 170 K for the lowest flyer velocity. It is considered that such transformation behaviour, depending on the flyer velocity, is

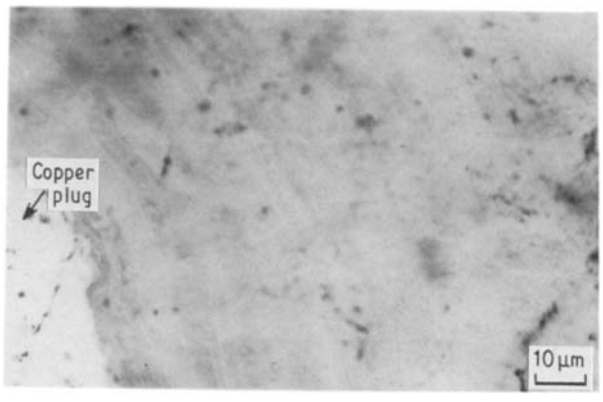

Figure 5 Optical micrograph of the peripheral part of the shock-loaded sample at a flyer velocity of 1.7 km sec^{-1}.

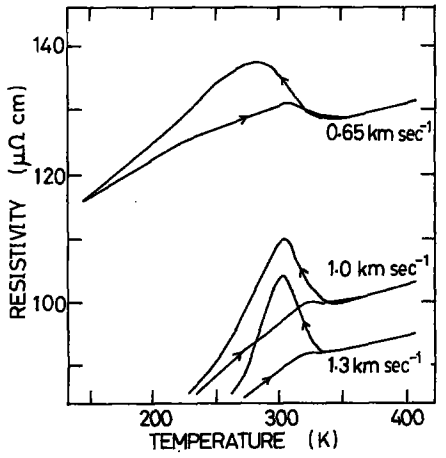

Figure 7 Electrical resistivity against temperature curves of the shock-compacted samples for flyer velocities of 0.65, 1.0 and 1.3 km sec^{-1}.

attributable to the differences of the internal stress in a minute portion. Alternatively, effects of the remarkable mechanical deformation and the annealing caused by the thermal energy deposited under the shock treatment evidently appear in the phase transition behaviour. The residual temperatures for the flyer velocities of 0.65, 1.0 and 1.3 km sec^{-1} are 570, 880 and 1200 K, respectively, as shown in Fig. 2. The relaxation time from the residual temperature to the ambient one is approximately estimated to be 50 msec by considering the thermal conduction for the present sample size. As this time is 10^3 times longer than the duration at which the shock pressure decays and the inhomogeneous shock temperature is relaxed to the homogeneous state, that relaxation time and the residual temperature can be regarded as an indicator for an annealing effect after shock loading. It can be speculated that the effect of the distortion intoduced by the plane shock wave is scarcely retained for the higher velocity impact, because the resistivity behaviour is similar to that for the NiTi alloys which are prepared by melting and undergo many thermal-cycles [23–25]. Consequently the influence of the marked deformation of particles, revealed as the broadening of the transformation region as shown in the resistivity behaviour for the flyer velocity of 0.65 km sec^{-1}, is decreased remarkably even by the annealing in temperatures over 880 K for a short time of 50 msec. Therefore, it is clear that the shock compaction of the NiTi powder sample accompanies effects of not only deforming but also annealing.

5. Conclusions

The shock recovery experiment for the NiTi powder sample with the initial density of 70% of the full density was performed by the flyer plate impact technique in the flyer velocity range from 0.65 to 1.7 km sec^{-1}, and the microstructures for the recovered samples were observed and the changes in electrical resistivity with temperature were measured. The shock state and the melted mass fraction were calculated on the basis of the Rankin–Hugoniot equations, the Mie–Grüneisen equation of state, etc. The relaxation of the temperature raised by the shock-loading was also estimated. A large fissure appears along the bottom of the shock-loaded sample, caused by the difference between the shock impedances of powder sample and the capsule in the present recovery assembly. The amount of melted region for the highest velocity increases remarkably because of the heat generation according to the marked deformation of shape, and prevents the shock compaction because of producing voids and cracks in the melted region. The porous sample obtained by the lowest velocity impact does not achieve an intergranular bonding, and initial voids remain on the particle surface. At the flyer velocity of 1.3 km sec^{-1} which is the best impact condition, the value of the density reaches up to 99.5% of the full density. The melted region is localized near the particle surface and increases with the flyer velocity. Although the calculated shock state for the best compaction is not so violent, i.e., the shock pressure of 13 GPa at the shock temperature of 1240 K, pores are produced in the melted region because of the small thermal conductivity of the NiTi alloy. The measured value on the melted mass fraction is in qualitative agreement with the calculated value except for the marked deformation sample. To estimate the melted mass fraction due to the marked deformation is very important, because not only uniaxial deformation for the compaction but also three-dimensional plastic deformation generates profuse heat. The shock treatment for the NiTi alloy powder exhibits effects of deforming and annealing which are characterized by the resistivity behaviour near the martensitic transformation temperature. The shock compacted sample is well annealed under the condition due to the heat generation and conduction for the flyer velocities above 1 km sec^{-1}. The annealing condition is in the temperatures over 880 K for a short time of 50 msec.

Acknowledgement

Thanks are due to Mr Kusaka of Daido Special Steel Co. Ltd. for supplying the alloy powder for this experiment.

References

1. W. H. GOURDIN, *J. Appl. Phys.* **55** (1984) 172.
2. W. H. GOURDIN and S. L. WEINLAND, in Proceedings of the American Physical Society Topical Conference on Shock Waves in Condensed Matter, Sante Fe, New Mexico, July 1983, edited by J. R. Asay, R. A. Graham and G. K. Straub, (Elsevier, New York, 1984) p. 99.
3. R. R. BOADE, *J. Appl. Phys.* **39** (1968) 5693.
4. R. R. BOADE, *ibid.* **41** (1970) 4542.
5. B. M. BUTCHER and C. H. KARNES, *ibid.* **40** (1969) 2967.
6. P. C. LYSNE and W. J. HALPIN, *ibid.* **39** (1968) 5488.
7. D. RAYBOULD, *J. Mater. Sci.* **16** (1981) 589.
8. G. M. MICHAL and R. SINCLAIR, *Acta Cryst.* **B37** (1981) 1803.
9. K. OTSUKA, T. SAWAMURA and K. SHIMIZU, *Phys. Stat. Sol. (a)* **5** (1971) 2769.
10. A. SAWAOKA and K. KONDO, *Report of the Research Laboratory of Engineering Materials, Tokyo Institute of Technology* **9** (1984) 131.
11. P. S. DECARLI and M. A. MAYERS, in "Shock Waves and High-Strain-Rate Phenomena in Metals" edited by M. A. Meyers and L. E. Murr (Plenum Press, New York 1981) p. 341.
12. R. G. McQUEEN, S. P. MARSH, J. W. TAYLOR,

J. N. FRITZ and W. J. CARTER, in "High-Velocity Impact Phenomena" edited by R. Kinslow (Academic Press, New York, 1970) p. 293.
13. J. E. GOFF, *J. Appl. Phys.* **35** (1964) 2919.
14. W. J. BUEHLER and R. C. WILEY, *Trans. Quart.* **55** (1962) 269.
15. N. G. PACE and G. A. SAUNDERS, *Phil. Mag.* **22** (1970) 73.
16. R. J. WASILEWSKI, S. R. BUTLER and J. E. HANLON, *Met. Sci. J.* **1** (1967) 104.
17. J. J. GILVARY, *Phys. Rev. Lett.* **16** (1966) 1089.
18. S. N. VAIDYA and E. S. R. GOPAL, *ibid.* **17** (1966) 635.
19. M. HANSEN, "Constitution of Binary Alloys" (McGraw-Hill, New York, 1958) p. 1049.
20. International Tables of Selected Constants 16, Metals, Thermal and Mechanical Data, edited by S. Allard (Pergamon, Oxford, 1969).
21. R. B. SCHWARZ, P. KASIRAJ, T. VREELAND Jr and T. J. AHRENS, *Acta Metall.* **32** (1984) 1243.
22. H. S. CARSLAW and J. C. JAEGER, "Conduction of Heat in Solids" 2nd Edn (Oxford University Press, Oxford, 1959) p. 242.
23. H. MATSUMOTO and S. DOHI, in Proceedings of the 27th Japan Congress on Materials Research, 1984 (Society of Materials Science, Kyoto) p. 1.
24. C. M. WAYMAN, I. CORNELIS and K. SHIMIZU, *Scripta Met.* **6** (1972) 115.
25. T. HONMA and H. TAKEI, *J. Jpn Inst. Metals* **39** (1975) 175 (in Japanese).

Received 3 April
and accepted 5 June 1986